Monatsh Chem (2010) 141:387–393
DOI 10.1007/s00706-010-0268-6

ORIGINAL PAPER

Synthesis, characterization, and anticancer properties of ferrocenyl complexes containing a salicylaldehyde moiety

Mokhles M. Abd-Elzaher · Samia A. Moustafa · Ammar A. Labib · Mamdouh M. Ali

Received: 16 June 2009 / Accepted: 11 February 2010 / Published online: 27 March 2010

Abstract A ferrocenyl ligand was prepared from condensation of 1,1′-diacetylferrocene dihydrazone with salicylaldehyde. This ligand forms 1:1 complexes with Co(II), Ni(II), Cu(II), and Zn(II) in good yield. Characterization of the ligand and complexes was carried out using infrared (IR), ^{1}H nuclear magnetic resonance (NMR), electronic absorption, and elemental analysis. Anticancer activity of the prepared ligand and its complexes against human breast cancer cell line MCF-7 was determined, and the results were compared with the activity of the commonly used anticancer drug cisplatin. Treatments of MCF-7 cells with gradually increasing doses (5, 10, 20, and 40 μg/cm^3) of the prepared complexes revealed that the activity of superoxide dismutase and the level of hydrogen peroxide were significantly increased, while the activities of catalase and glutathione peroxidase and the levels of reduced glutathione were significantly lowered compared with in MCF-7 cells harvested from control. The results suggested that the prepared compounds possess significant anticancer activity comparable to the activity of cisplatin and may be potent anticancer agents for inclusion in modern clinical trials.

Keywords Bioinorganic chemistry · Ligands · Metallocenes · Schiff bases · Transition-metal compounds

M. M. Abd-Elzaher (✉) · S. A. Moustafa · A. A. Labib
Inorganic Chemistry Department, National Research Centre, Dokki, Cairo, 12622, Egypt
e-mail: mokhlesm20@yahoo.com

M. M. Ali
Biochemistry Department, National Research Center, Dokki, Cairo, 12622, Egypt

Introduction

Use of ferrocene in bioorganometallic chemistry has been growing rapidly in recent years. This may be because ferrocenyl derivatives are stable compounds, nontoxic, and have good redox properties. Many ferrocenyl compounds display interesting antitumor [1–4], antimalarial [5–7], antifungal [8, 9], and DNA-cleaving activity [10–12]. Along this line, Jaouen et al. prepared several derivatives of ferrocifen based on the structure of tamoxifen and hydroxytamoxifen. The series of ferrocifens were biologically examined in vitro and in vivo, and the results [13, 14] showed that ferrocifens are active against both hormone-dependent and hormone-independent breast cancer cells. Jaouen et al. [15] investigated also several derivatives of polyphenolic compounds containing a ferrocene moiety and evaluated them as anticancer agents using standard breast cancer cell lines.

Another successful example is a ferrocene-chloroquine analogue, i.e., ferrochloroquine (FQ, 7-chloro-4-[2-(*N*′,*N*′-dimethylaminomethyl)-*N*-ferrocenylmethylamino]quinoline), in which one ferrocene unit was integrated into chloroquine (CQ). In vitro, FQ proved to be about 22 times more biologically active than CQ against chloroquine-resistant strains of *P. falciparum* and showed higher activity in vivo in mice infected with *P. berghei* N and *P. yoelii* NS [3, 16, 17].

Also, the redox properties of ferrocene have been exploited to prepare different types of electrochemical sensors such as DNA, protein, environmental pollutant, and food sensors, and this area of research is growing rapidly [18, 19].

These interesting applications of ferrocenyl compounds have attracted the attention of many authors to study heterobimetallic complexes [20–22], since some ferrocenyl complexes showed more biological activity than the parent

ligand. The aim of this work is to prepare and characterize a ferrocenyl ligand derived from condensation of 1,1′-diacetylferrocene dihydrazone with salicylaldehyde. The ligand **1** has been well characterized using different spectroscopic techniques. The study was extended to prepare and characterize Co(II), Ni(II), Cu(II), and Zn(II) complexes with the mentioned ligand to obtain the heterobimetallic complexes **2–5**. Ligand **1** and its complexes **2–5** have been characterized by IR, ^{1}H NMR, UV–Vis spectra as well as elemental analysis. On the other hand, platinum compounds such as cisplatin, carboplatin, and oxaliplatin are some of the most potent anticancer drugs available today. These compounds are used for treatment of different cancer types, although they have several severe side-effects [23]. Preparing new compounds with improved potency or wide specificity is among the major targets for pharmaceutical companies. Therefore, our aim was extended to study the anticancer activity of ligand **1** and complexes **2–5**, hoping to compare their activity with that of cisplatin.

Results and discussion

*Synthesis and characterization of ligand **1***

1,1′-Diacetylferrocene dihydrazone was prepared by reacting 1,1′-diacetylferrocene, dissolved in a small amount of dry ethanol, with an excess of hydrazine hydrate while stirring under nitrogen. The deep-brown color of the diacetylferrocene started to change to orange within the first 4–6 h, but stirring was continued to complete the reaction. Characterization of ferrocenyl dihydrazone was carried out using IR, NMR, and UV–Vis spectra. The IR spectra of the prepared dihydrazone showed a medium band at 1,659 cm^{-1}, which was assigned to the formation of the C=N group [20, 21]. In addition, the frequency of the two NH_2 groups appeared as a broad band at about 3,340 and 3,205 cm^{-1} [24]. This result was confirmed by the broad ^{1}H NMR band at 5.08 ppm, which was assigned to the NH_2 groups of the 1,1′-diacetylferrocene dihydrazone.

The ligand **1** (Fig. 1) was prepared by addition of salicylaldehyde to 1,1′-diacetylferrocene dihydrazone in ethanol under reflux for 4 h. The color of the dihydrazone was changed to orange-red. The ligand **1** was isolated in good yield and is soluble in common organic solvents such as ethanol, methanol, acetone, and chloroform. Structure of **1** was confirmed by IR spectra. The band at 1,615 cm^{-1} due to N=C was found to become stronger and broader [21]. This may be due to the formation of another two N=C bonds in the ligand. A broad band centered at 3,430 cm^{-1} indicated the presence of the OH group in the ligand. The

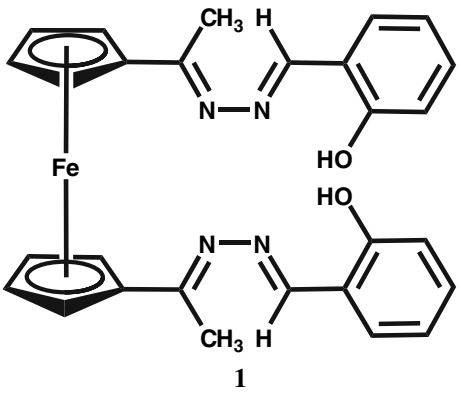

1

Fig. 1 Structure of the ligand **1**

breadth of this band also suggested the presence of hydrogen bonding between the azomethine nitrogen and the OH group [25]. A broad band centered at 1,042 cm^{-1} was observed with medium intensity and was assigned to the N–N group [26]. In the ^{1}H NMR, the protons of the cyclopentadienyl groups appeared at 4.9 and 4.6 ppm. The phenyl protons were noticed as new bands at 6.9–7.5 ppm. The proton in the H–C=N group appeared as a singlet at 8.6 ppm, whereas the phenolic OH appeared at 9.8 ppm in the ^{1}H NMR. This peak was confirmed from other ^{1}H NMR spectra of similar Schiff bases [20, 21].

*Synthesis and characterization of the complexes **2–5***

The complexes of cobalt(II), nickel(II), copper(II), and zinc(II) ions were prepared easily and in good yield from an equimolar ratio of **1** and the corresponding metal(II) chloride in ethanol under reflux. All the complexes **2–5** are deep red, which may be due to conjugation of the ligand with the metal ions. The complexes **2–5** are also stable in air and under light, and are soluble in dimethylformamide (DMF) and dimethyl sulfoxide (DMSO). Elemental analysis showed that **2–5** have 1:1 (metal:ligand) molar ratio.

The IR spectra of **1–5** were recorded as KBr pellets. It was found that the characteristic band of the C=N group in the free ligand **1** (at 1,615 cm^{-1}) was shifted to lower frequency of 1,602–1,606 cm^{-1} in the complexes **2–5** [21]. This shift indicates coordination of the azomethine nitrogen to the metals in the complexes. It was also found that the medium band due to N–N in **1** (at 1,042 cm^{-1}) was shifted to lower frequency (1,024–1,030 cm^{-1}) in **2–5** [21]. This shift indicates that bonding in the complexes occurred through the nitrogen atom.

In the low-frequency region, two bands were observed for **2–5** at 450 and 465 cm^{-1}, which were attributed to ν(M–N) and ν(M–O), respectively. These bands were not found in the spectra of **1**, suggesting that coordination of the ligand with the metal ions takes place via the

azomethine nitrogen atoms and also via the deprotonated phenolic oxygen [20, 27].

The characteristic frequencies of the ferrocenyl moiety in the spectra of **1** were observed at about 3,078, 1,412, 1,111, 1,005, 817, and 490 cm^{-1}. The band at 3,078 cm^{-1} was assigned to the C–H stretching band. The band at 1,412 cm^{-1} was assigned to the asymmetric C–C stretching band. The 1,111 cm^{-1} band was due to asymmetric ring-breathing vibration. The two bands located at 1,005 and 817 cm^{-1} were assigned to parallel and perpendicular C–H bands, respectively. The final band at 490 cm^{-1} was assigned to the Fe–Cp stretching frequency [20–22]. The corresponding frequencies of the complexes appeared at nearly the same position, which indicates that the cyclopentadienyl ring of the ferrocene is not directly coordinated to the metal ion [20–22].

^{1}H NMR spectra

NMR spectra of **1–5** were recorded in DMSO-d_6 at room temperature using tetramethylsilane (TMS) as internal standard. All ^{1}H NMR spectra showed two multiplets for the α- and β-protons of the cyclopentadienyl rings at 4.7 and 4.4 ppm [20–22, 26]. The signals of the methyl groups were observed at 2.2 ppm in **1**. These signals were shifted slightly downfield in the spectra of **2–5**, which may be due to complexation of the azomethine nitrogens with the metal ion.

The signal observed for the OH protons of **1** (ca. 9.7 ppm) was not observed in any of the complexes **2–5**, which confirms the bonding of the phenolic oxygen to the metal ions (C–O–M) [20, 27]. The signals of the phenyl protons in **1** and also in **2–5** were found in the expected regions at 7.59–6.82 ppm.

Electronic spectra

The electronic spectrum of the Co(II) complex **2** consists of two shoulder bands at 578 and 484 nm. These bands are assigned to the transitions $^4T_{1g}(F) \rightarrow {}^4A_{2g}(F)$ and $^4T_{1g}(F) \rightarrow {}^4T_{2g}(P)$, respectively, and are characteristic for high-spin octahedral geometry of Co(II) complexes (Fig. 2) [27, 28]. On the other hand, the spectrum of the nickel(II) complex **3** consists of two bands at 534 and 496 nm. These bands are attributed to the $b_{2g} \rightarrow b_{1g}$ and $a_{1g} \rightarrow b_{1g}$ transitions, which is compatible with complexes having a square-planar structure [29, 30]. In the spectra of the Cu(II) complex **4** three bands at 659, 510, and 329 nm were observed. The first two bands are assigned to $^2B_{1g} \rightarrow {}^2A_{1g}$ and $^2B_{1g} \rightarrow {}^2E_g$ transitions, respectively [27, 31]. These bands are typically characteristic for square-planar configuration (Fig. 3). The third band is assigned to metal–ligand charge transfer. The electronic spectra of the

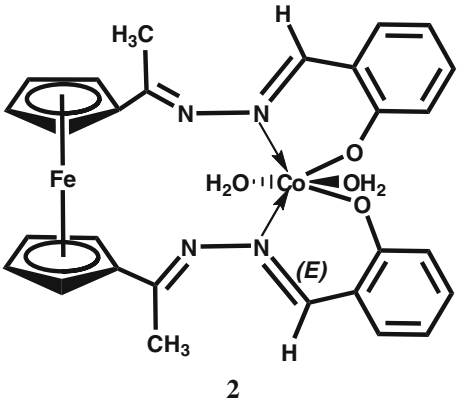

2

Fig. 2 Structure representation of the Co complex **2**

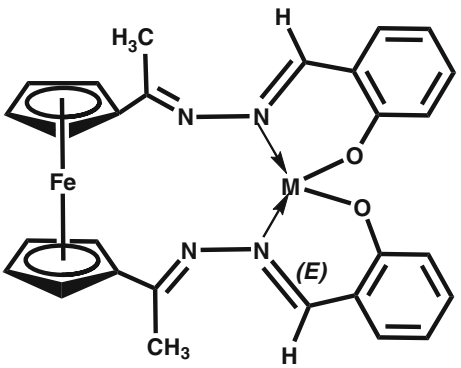

3, **4**, **5**
M = Ni, Cu, Zn

Fig. 3 Structure representation of the Ni, Cu, and Zn complexes **3-5**

Zn(II) complexes **5** showed one high-intensity band at 350 nm, which is assigned to ligand–metal charge transfer [27, 31].

A weak, broad band was also observed for **2–5** at 443–448 nm. This band was assigned to the transition $^1A_{1g} \rightarrow {}^1E_{1g}$ in the iron atom of the ferrocenyl group, which indicates that there is no magnetic interaction between the Co(II), Ni(II), Cu(II), and Zn(II) ions and the Fe(II) ion of the ferrocenyl group [20, 21, 26].

On the basis of the spectral data of the complexes discussed above, one can assume that the metal ions are bonded to the ligand via the nitrogen and the phenolic oxygen atom in all complexes **2–5** (Figs. 2, 3).

*Anticancer activity of **1–5***

Compounds **1–5** were screened in vitro using a single tumor (MCF-7 cells). Cells exposed to different concentrations of the tested compounds exhibited a dose-dependent reduction of 3-(4,5-dimethylthiazol-2-yl)-2,5-diphenyltetrazolium bromide (MTT), revealing preservation of viability in the presence of the tested compounds (Fig. 4). The doses of

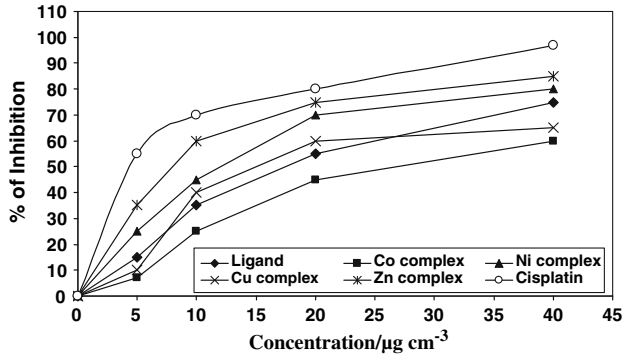

Fig. 4 Effect of different concentrations of the prepared compounds on MCF-7 cell growth, measured by MTT assay

the tested compounds were selected based on the preliminary studies.

The tumor cell line showed normal growth in our culture system. DMSO did not seem to have any noticeable effect on cellular growth. A gradual decrease in viability of cancer cells was observed with increasing concentration of the tested compounds, in a dose-dependent inhibitory effect. The Zn complex **5** was the best compound, exerting a significant cytotoxic effect on MCF-7 cells compared with cisplatin.

The median growth inhibitory concentration (IC_{50}) after 24 h was 17.50 μg/cm^3 for **1**, 26.50 μg/cm^3 for **2**, 12.00 μg/cm^3 for **3**, 15.00 μg/cm^3 for **4**, and 8.10 μg/cm^3 for **5**.

To elucidate the mechanism by which the prepared complexes exert their antitumor activities, we estimated the activities of the free-radical-metabolizing enzymes superoxide dismutase (SOD), catalase (CAT), and glutathione peroxidase (GSH-Px), as well as the levels of glutathione (GSH) and H_2O_2 in MCF-7 cells. As shown in Table 1, treatment of the cells with the ligand and its complexes increased the activity of SOD and the level of H_2O_2 (in dose-dependent manner) as compared with the control. In addition, our results revealed that treatment with **2**–**5** leads to decrease in the activity of CAT and GSH-Px as well as the level of GSH (in dose-dependent manner).

The results showed that the order of antitumor activity of the compounds was: **5** > **3** > **1** > **4** > **2**. The highest activity was found for Zn and Ni complexes, which resulted in the highest SOD activity and H_2O_2 and low activities of CAT and GSH-Px as well as GSH level. These results indicate that the antitumor effect of the present complexes may be exerted at least partly by production of H_2O_2.

The mode of action of **1**–**5** is still unclear. The antitumor activities are accompanied by dose-dependent increases in SOD activities of treated cells compared with the control group. This means that **1**–**5** can cause H_2O_2 production. The H_2O_2 produced should be rapidly removed through the activation of CAT and GSH-Px. The present results show that activities of CAT and GSH-Px and the level of reduced GSH are lowered in groups treated with **1**–**5** (in dose-dependent manner) compared with the control group (Table 1).

Consequently, the excess H_2O_2 produced in tumor cells with **1**–**5** cannot be removed. In other words, the accumulation of H_2O_2 in tumor cells should be partly the cause of tumor cell death. Thus the results of the present study are consistent with the hypothesis that **1**–**5** exert their antitumor effects through production of reactive oxygen species (ROS).

The previous results were confirmed by the fact that most chemotherapeutic agents cause cells to overgenerate ROS [32], so they are capable of inducing apoptosis, and oxidative damage to DNA, proteins, and lipids. The cascade of signals mediating apoptosis often involves a ROS intermediate messenger, and ROS can short-circuit the pathway, bypassing the need for upstream signals for cell suicide. Recently, Huang et al. [33] observed that selective inhibition of SOD kills human cancer cells but not normal cells, suggesting that regulation of free-radical-producing agents may also have important clinical applications. This mechanism for the effects of ROS-generating anticancer agents is only beginning to be understood, as previously the mechanism of most anticancer agents was believed to be due mainly to direct interaction with DNA and interference with DNA regulatory machinery (e.g., topoisomerases, helicases) and to initiation of DNA damage via production of ROS [34].

Moreover the Zn complex **5** showed the highest antitumor activity, and this can be explained by the fact that zinc is an essential trace element, has important biological functions, and is used to cure various ailments, including growth failure, cancer, infection, and skin diseases [35]. In a previous study it has been mentioned that Ni complexes were reported as promising cytotoxic and antimicrobial agents [36].

In conclusion, the present results suggest that the prepared compounds possess significant anticancer activity, comparable to the activity of the commonly used anticancer drug cisplatin. These complexes may exert their antitumor activities partly by increasing hydrogen peroxide production and by depletion of intracellular catalase, glutathione peroxidase, and reduced glutathione. The results revealed that these complexes may be potent anticancer agents for inclusion in modern clinical trials.

Experimental

All chemicals and solvents were obtained from Merck. 1,1′-Diacetylferrocene was prepared according to Ref. [37],

Table 1 Effect of treatment with different concentrations of **1**–**5** on the activities of superoxide dismutase (SOD), catalase (CAT), and glutathione peroxidase (GSH-Px) as well as the levels of reduced glutathione (GSH) and hydrogen peroxide (H_2O_2) in MCF-7 cells

Treatment ($\mu g/cm^3$)	SOD (U/mg protein)	CAT (U/mg protein)	GSH-Px (U/mg protein)	GSH (nmol/mg protein)	H_2O_2 (nmol/mg protein)
Control	30.45 ± 4.11	8.80 ± 0.50	9.50 ± 0.70	37.70 ± 3.20	11.70 ± 1.60
Cisplatin					
5	120.85 ± 13.40	3.11 ± 0.40	4.30 ± 0.48	16.90 ± 1.85	33.60 ± 3.61
10	140.33 ± 15.00	2.80 ± 0.30	3.43 ± 0.39	15.70 ± 1.75	55.20 ± 5.80
20	360.60 ± 24.80	2.44 ± 0.25	2.16 ± 0.25	15.11 ± 2.00	67.75 ± 7.11
40	410.80 ± 35.89	1.50 ± 0.11	1.60 ± 0.2	13.20 ± 1.80	80.50 ± 7.60
1					
5	49.50 ± 5.20	5.00 ± 0.40	7.10 ± 0.65	23.80 ± 2.50	20.45 ± 1.80
10	84.12 ± 9.13	4.24 ± 0.36	6.12 ± 0.60	22.45 ± 2.60	33.75 ± 3.90
20	110.75 ± 12.00	3.65 ± 0.25	5.33 ± 0.61	19.45 ± 2.00	38.11 ± 4.00
40	220.70 ± 25.63	2.90 ± 0.30	4.80 ± 0.50	17.66 ± 1.90	43.73 ± 4.50
2					
5	35.55 ± 4.11	6.60 ± 0.70	8.63 ± 0.90	30.12 ± 3.62	15.90 ± 1.75
10	66.75 ± 6.50	5.70 ± 0.63	7.36 ± 0.83	25.16 ± 2.80	22.70 ± 2.50
20	82.00 ± 7.90	5.26 ± 0.60	6.00 ± 0.55	21.65 ± 2.60	25.34 ± 3.00
40	145.67 ± 16.00	3.82 ± 0.40	5.11 ± 0.45	19.65 ± 2.11	29.53 ± 3.11
3					
5	65.40 ± 7.00	4.55 ± 0.53	6.63 ± 0.70	21.80 ± 0.24	25.33 ± 2.40
10	110.20 ± 10.42	4.10 ± 0.39	5.60 ± 0.62	20.86 ± 0.20	38.67 ± 4.00
20	140.00 ± 13.80	3.22 ± 0.33	3.11 ± 0.40	19.70 ± 0.17	41.87 ± 4.70
40	290.17 ± 30.00	2.20 ± 0.19	2.65 ± 0.25	19.00 ± 0.21	53.14 ± 5.50
4					
5	40.33 ± 4.14	5.30 ± 0.61	7.50 ± 0.82	25.20 ± 2.87	19.34 ± 1.76
10	75.80 ± 8.00	4.80 ± 0.50	7.00 ± 0.65	22.85 ± 2.90	26.60 ± 3.00
20	101.75 ± 11.00	4.70 ± 0.37	6.33 ± 0.55	17.30 ± 2.00	27.75 ± 3.40
40	120.40 ± 9.85	3.26 ± 0.36	5.65 ± 0.70	16.11 ± 2.35	36.50 ± 4.11
5					
5	101.90 ± 13.90	3.85 ± 0.20	5.11 ± 0.72	19.87 ± 2.00	28.23 ± 3.11
10	130.40 ± 8.70	3.36 ± 0.42	4.90 ± 0.50	19.12 ± 0.24	45.45 ± 3.90
20	320.80 ± 22.79	2.76 ± 0.17	3.70 ± 0.43	17.11 ± 0.18	50.85 ± 6.00
40	360.60 ± 34.00	1.75 ± 0.11	2.22 ± 0.18	15.00 ± 1.68	67.33 ± 6.13

Data are expressed as mean ± standard error (SE) of four separate experiments. All values for **1**–**5** and cisplatin were significantly different at $p < 0.05$ versus control

and 1,1′-diacetylferrocene dihydrazone was synthesized as described in Ref. [21]. Yields refer to analytically pure compounds and were not optimized. ^{1}H NMR was recorded with a JEOL EX-270 MHz FT NMR spectrometer in DMSO-d_6 as solvent. IR spectra were recorded on a Perkin Elmer (Spectrum 1000) Fourier-transform infrared (FT-IR) spectrometer, using KBr pellets. Elemental analyses were determined at the Microanalytical Center, Cairo University, and the results agreed favorably with calculated values. Electronic absorptions were recorded on a Shimadzu UV240 automatic spectrophotometer in DMSO.

1,1′-Bis[1-[2-[(2-hydroxyphenyl)methylene]hydrazinylidene]ethyl]ferrocene (**1**, $C_{28}H_{26}FeN_4O_2$)

Salicylaldehyde (2.30 cm^3, 22 mmol) was slowly added to a magnetically stirred solution of 2.98 g 1,1′-diacetylferrocene dihydrazone (10 mmol) in 50 cm^3 methanol. The mixture was refluxed for 4 h. Concentration of the solution to the appropriate volume and cooling to 5 °C yielded **1**. The solid was filtered off, washed with cold methanol, and dried. Yield 72%; IR (KBr): $\bar{\nu} = 3{,}425$ (O–H), 1,287 (C–O), 1,615 (C=N), 1,042 (N–N) cm^{-1}; ^{1}H NMR (270 MHz, DMSO-d_6): $\delta = 2.21$ (s, 6H, $2CH_3$), 4.38 (m,

4H, C_5H_4), 4.65 (m, 4H, C_5H_4), 7.56–6.82 (m, 8H, Ph), 8.61 (s, 2H, CH=N), 9.72 (s, 2H, OH) ppm.

*General procedure for synthesis of complexes **2–5***

Complexes **2–5** were prepared by addition of 2.0 mmol $CoCl_2{\cdot}6H_2O$, $NiCl_2{\cdot}6H_2O$, $CuCl_2{\cdot}2H_2O$, or $ZnCl_2$ dissolved in ca. 20 cm^3 ethanol to a warmed solution of 2.0 mmol **1** in 50 cm^3 ethanol. The mixture was refluxed for 4 h. The complex precipitated on cooling to 5 °C, was filtered off, washed two times with cold ethanol, and dried.

[(Ferrocene-1,1′-diyl)bis[2-[(2-ethylidenhydrazinyliden-κN2)methyl]phenolato]cobalt dihydrate
(**2**, $C_{28}H_{28}CoFeN_4O_4$)
Yield 73%; IR (KBr): $\bar{\nu}$ = 3,411 (O–H), 1,605 (C=N), 1,310 (C–O), 1,026 (N–N), 465 (M–O), 452 (M–N) cm^{-1}; UV–Vis (MeOH): λ_{max} = 578, 484, 443 nm.

[(Ferrocene-1,1′-diyl)bis[2-[(2-ethylidenhydrazinyliden-κN2)methyl]phenolato]nickel (**3**, $C_{28}H_{24}FeN_4NiO_2$)
Yield 71%; IR (KBr): $\bar{\nu}$ = 3,400 (O–H), 1,603 (C=N), 1,318 (C–O), 1,024 (N–N), 463 (M–O), 447 (M–N) cm^{-1}; ^{1}H NMR (270 MHz, DMSO-d_6): δ = 2.23 (s, 6H, $2CH_3$), 4.36 (m, 4H, C_5H_4), 4.68 (m, 4H, C_5H_4), 7.57–6.84 (m, 10H, Ph), 8.66 (s, 2H, CH=N) ppm; UV–Vis (MeOH): λ_{max} = 534, 496, 448 nm.

[(Ferrocene-1,1′-diyl)bis[2-[(2-ethylidenhydrazinyliden-κN2)methyl]phenolato]copper (**4**, $C_{28}H_{24}CuFeN_4O_2$)
Yield 74%; IR (KBr): $\bar{\nu}$ = 1,602 (C=N), 1,324 (C–O), 1,028 (N–N), 462 (M–O), 444 (M–N) cm^{-1}; UV–Vis (MeOH): λ_{max} = 659, 510, 446, 329 nm.

[(Ferrocene-1,1′-diyl)bis[2-[(2-ethylidenhydrazinyliden-κN2)methyl]phenolato]zinc (**5**, $C_{28}H_{24}FeN_4O_2Zn$)
Yield 70%; IR (KBr): $\bar{\nu}$ = 3,436 (O–H), 1,606 (C=N), 1,311 (C–O), 1,030 (N–N), 465 (M–O), 442 (M–N) cm^{-1}; ^{1}H NMR (270 MHz, DMSO-d_6): δ = 2.22 (s, 6H, $2CH_3$), 4.40 (m, 4H, C_5H_4), 4.67 (m, 4H, C_5H_4), 7.59–6.83 (m, 10H, Ph), 8.67 (s, 2H, CH=N) ppm; UV–Vis (MeOH): λ_{max} = 444, 350 nm.

Cell culture

The human breast cancer cell line MCF-7 was maintained in Dulbecco's modified Eagle's medium (DMEM) supplemented with 10% heat-inactivated fetal calf serum (GIBCO), penicillin (100 U/cm^3), and streptomycin (100 μg/cm^3) at 37 °C in humidified atmosphere containing 5% CO_2. Cells at concentration of 0.50 × 10^6 were grown in a 25-cm^3 flask in 5 cm^3 complete culture medium.

Estimation of in vitro tumor cell growth inhibition was assessed by incubating 0.65 × 10^5 MCF-7 cells in 1 cm^3 phosphate buffer saline with varying concentrations of **1–5** and cisplatin (as a positive control drug) at 37 °C for 24 h in CO_2 atmosphere. Cells were cultured for 24 h to ensure total attachment. Afterwards, the tested compounds were added to the cells. Cell survival was evaluated at the end of the incubation period by MTT colorimetric assay. In all cellular experiments results were compared with untreated cells.

Cytotoxicity assay

The effect of **1–5** on growth of MCF-7 cells was estimated by MTT colorimetric assay [38]. This method is based on the selective ability of living cells to reduce the yellow soluble salt of MTT to a purple-blue insoluble formazan precipitate. The number of viable cells is proportional to the production of formazan salts. The crystals of formazan were dissolved in DMSO, and the optical density was measured spectrophotometrically (Microplates reader; Asys Hitech, Austria).

Cells (0.65 × 10^5 cells/well) were plated separately in a sterile flat-bottomed 96-well microplate (Falcon) and treated with 20 mm^3 of different concentration of **1–5** and cisplatin (5, 10, 20, or 40 μg/cm^3) for 24 h at 37 °C in a humidified 5% CO_2 atmosphere. Then, incubation media were removed and 40 mm^3 MTT solution/well was added and incubated for an additional 4 h. MTT crystals were solubilized by adding 200 mm^3 DMSO/well, and the plate was shaken gently for 10 min at room temperature. The results were determined photometrically using a microplate enzyme-linked immunosorbent assay (ELISA) reader and absorbance at 570 nm. Data are expressed as percentage relative viability compared with untreated cells, calculated using the following equation:

$$(\text{Absorbance of treated cells})/(\text{absorbance of control cells}) \times 100.$$

The cytotoxic concentration was expressed by half maximal IC_{50}. IC_{50} calculations were performed using Microsoft Excel and Microcal Origin software for PC.

Antioxidants status assay

Enzyme activities and the level of both reduced glutathione (GSH) and lipid peroxidation (LP) were expressed in cell lysates as a function of total cellular protein [39]. Activities of SOD, CAT, and GSH-Px were determined as described in literature [40–42]. Levels of reduced glutathione (GSH) and hydrogen peroxide (H_2O_2) were determined using the methods of Ellman [43] and Wolf [44].

Statistical analysis

The results are reported as mean ± standard error (SE) for at least four experiments. Statistical differences were analyzed using one-way analysis of variance (ANOVA) test followed by Student's t test, wherein differences were considered significant at $p < 0.05$.

Acknowledgment The author M.M.A. would like to thank Alexander von Humboldt Foundation for providing equipment.

References

1. Fouda MFR, Abd-Elzaher MM, Abdelsamaia RA, Labib AA (2007) Appl Organomet Chem 21:613
2. Popova LV, Babin VN, YuA Belousov, YuS Nekrasov, Snegireva AE, Borodina NP, Shaposhnikova GM, Bychenko OB, Raevskii PM, Morozova NB, Iiyina AI, Shitkov KG (1993) Appl Organomet Chem 7:85
3. Henderson W, Alley SR (2001) Inorg Chim Acta 322:106
4. Michard Q, Jaouen G, Vessieres A, Bernard BA (2008) J Inorg Biochem 102:1980
5. Suresh Babu AR, Raghunathan R (2008) Tetrahedron Lett 49:4487
6. Biot C, Pradines B, Sergeant M-H, Gut J, Rosenthal PJ, Chibale K (2007) Bioorg Med Chem Lett 17:6434
7. Daher W, Biot C, Fandeur T, Jouin H, Pelinski L, Viscogliosi E, Fraisse L, Pradines B, Brocard J, Khalife J, Dive D (2006) Malar J 5:11
8. Chohan ZH (2006) Appl Organomet Chem 20:112
9. Chantson JT, Falzacappa MVV, Crovella S, Metzler-Nolte N (2005) J Organomet Chem 690:4564
10. Maity B, Roy M, Chakravarty AR (2008) J Organomet Chem 693:1395
11. Pan X-H, Liu X, Zhao B-X, Xie Y-S, Shin D-S, Zhang S-L, Zhao J, Miao J-Y (2008) Bioorg Med Chem 16:9093
12. Sato S, Nojima T, Takenaka S (2004) J Organomet Chem 689:4722
13. Vessieres A, Top S, Beck W, Hillarda E, Jaouen G (2006) Dalton Trans 529
14. Top S, Vessieres A, Leclercq G, Quivy J, Tang J, Vaissermann J, Huche M, Jaouen G (2003) Chem Eur J 9:5223
15. Vessieres A, Top S, Pigeon P, Hillard E, Boubeker L, Spera D, Jaouen G (2005) J Med Chem 48:3937
16. Domarle O, Blampain G, Agnanet H, Nzadiyabi T, Lebibi J, Brocard J, Maciejewski L, Biot C, Georges AJ, Millet P (1998) Antimicrob Agents Chemother 42:540
17. Biot C, Delhaes L, Diaye CMN, Maciejewski LA, Camus D, Dive D, Brocard JS (1999) Bioorg Med Chem 7:2843
18. Zhao G-C, Xu M-Q, Zhang Q (2008) Electrochem Commun 10:1924
19. Sato N, Okuma H (2008) Sens Actuators B Chem 129:188
20. Abd-Elzaher MM (2004) Appl Organomet Chem 18:149
21. Abd-Elzaher MM, Hegazy W, Gaafar A (2005) Appl Organomet Chem 19:911
22. Abd-Elzaher MM, Ali IAI (2006) Appl Organomet Chem 20:107
23. Wheate NJ, Collins JG (2003) Coord Chem Rev 241:133
24. Fang CJ, Duan CY, Mo H, He C, Meng QJ, Liu YJ, Mei YH, Wang ZM (2001) Organometallics 20:2525
25. Dudeja M, Malhotra R, Dhindsa KS (1993) Synth React Inorg Met Org Chem 23:921
26. El-Shiekh SM, Abd-Elzaher MM, Eweis M (2006) Appl Organomet Chem 20:505
27. Chohan ZH, Praveen M (2001) Appl Organomet Chem 15:617
28. Chohan ZH, Pervez H, Kausar S, Supuran CT (2002) Synth React Inorg Met Org Chem 32:529
29. Atkins R, Breweg G, Kakot E, Mockler GM, Sinn E (1985) Inorg Chem 24:127
30. Mockler GM, Chaffey GW, Sin E, Wong H (1972) Inorg Chem 11:1308
31. Lever ABP (1984) Inorganic electronic spectroscopy. Elsevier, Amsterdam, pp 555–572
32. Bienvenu P, Caron L, Gasparutto D, Kergonou JF (1992) EXS 62:257
33. Huang P, Feng L, Oldham EA, Keating MJ, Plunkett W (2000) Nature 407:390
34. Gewirtz DA (1999) Biochem Pharmacol 57:727
35. Shah DR, Singh PP, Gupta RC, Bhandari TK (1988) Ind J Physiol Pharm 32:47
36. Yadrick MK, Kenney MA, Winterfeldt EA (1989) Am J Clin Nutr 49:145
37. Rosenblum M, Woodward RB (1958) J Am Chem Soc 80:5443
38. Mosmann T (1983) J Immunol Methods 65:55
39. Lowry OH, Rosebrough NJ, Farr AL, Randall RJ (1951) J Biol Chem 193:265
40. Paglia ED, Valentine WN (1967) J Lab Clin Med 70:158
41. Aebi H (1984) Catalase. In: Methods of enzymatic analysis, vol 2. Academic Press, New York, pp 673–684
42. Marklund S, Marklund G (1974) Eur J Biochem 47:469
43. Ellman GL (1959) Arch Biochem Biophys 82:70
44. Wolf SP (1994) Meth Enzymol 233:182